HHS Public Access

Author manuscript

*Diabetologia*. Author manuscript; available in PMC 2018 April 01.

Published in final edited form as:

*Diabetologia*. 2017 April ; 60(4): 740–750. doi:10.1007/s00125-017-4214-6.

# Enhanced VEGF signalling mediates cerebral neovascularisation via downregulation of guidance protein ROBO4 in a rat model of diabetes

**Mohammed Abdelsaid**[1,2], **Maha Coucha**[1,2], **Sherif Hafez**[1,2], **Abdul Yasir**[1,2], **Maribeth H. Johnson**[3], and **Adviye Ergul**[1,2]

[1]Charlie Norwood Veterans Administration Medical Center, Augusta, GA, USA

[2]Department of Physiology, Augusta University, 1120 15th Street CA-3135, Augusta, GA 30912, USA

[3]Department of Biostatistics, Augusta University, Augusta, GA, USA

## Abstract

**Aims/hypothesis—**Diabetes promotes cerebral neovascularisation via increased vascular endothelial growth factor (VEGF) angiogenic signalling. Roundabout-4 (ROBO4) protein is an endogenous inhibitor of VEGF signalling that stabilises the vasculature. Yet, how diabetes affects ROBO4 function remains unknown. We hypothesised that increased VEGF signalling in diabetes decreases ROBO4 expression and function via binding of ROBO4 with VEGF-activated β3 integrin and that restoration of ROBO4 expression prevents/repairs cerebral neovascularisation in diabetes.

**Methods—**ROBO4 protein expression in a rat model of type 2 diabetes (Goto–Kakizaki [GK] rats) was examined by western blotting and immunohistochemistry. ROBO4 was locally overexpressed in the brain and in primary brain microvascular endothelial cells (BMVECs). GK rats were treated with SKLB1002, a selective VEGF receptor-2 (VEGFR-2) antagonist. Cerebrovascular neovascularisation indices were determined using an FITC vascular space-filling model. Immunoprecipitation was used to determine ROBO4–β3 integrin interaction.

**Results—**ROBO4 expression was significantly decreased in the cerebral vasculature as well as in BMVECs in diabetes ($p<0.05$). Silencing *Robo4* increased the angiogenic properties of control BMVECs ($p<0.05$). In vivo and in vitro overexpression of ROBO4 inhibited VEGF-induced angiogenic signalling and increased vessel maturation. Inhibition of VEGF signalling using SKLB1002 increased ROBO4 expression ($p<0.05$) and reduced neovascularisation indices

Corresponding author: M. Abdelsaid, Department of Physiology, Augusta University, 1120 15th Street CA-3135, Augusta, GA 30912, USA, mabdelsaid@augusta.edu.

**Data availability**

The data are available on request from the authors.

**Duality of interest**

The authors declare that there is no duality of interest associated with this manuscript.

**Contribution statement**

MA, MC, SH and AY contributed to conception, design and acquisition of data. MHJ contributed to statistical analysis. MA and AE contributed to data analysis and interpretation. MA, MC, SH, AY, MHJ and AE contributed to drafting, revising and approving the manuscript for final publication. MA is the guarantor of this work.

($p<0.05$). Furthermore, SLKB1002 significantly decreased ROBO4–β3 integrin interaction in diabetes ($p<0.05$).

**Conclusions/interpretation—**Our study identifies the restoration of ROBO4 and inhibition of VEGF signalling as treatment strategies for diabetes-induced cerebral neovascularisation.

### Keywords

Angiogenesis; Anti-VEGF; Brain neovascularisation; Diabetes; ROBO4 signalling; VEGF signalling

## Introduction

Diabetes increases the risk and amplifies the severity of cerebral disorders including stroke and cognitive decline [1]. Accelerated macrovascular disease and atherosclerosis contribute to these complications in diabetes [2]. There is growing evidence that microvascular disease may also be involved. Microangiopathy, functional and structural dysfunction associated with small vessels, is a primary factor in the development and progression of diabetes-related disabilities including blindness, kidney failure and peripheral neuropathy [1–6]. Yet, the effects of diabetes on the cerebral microvasculature are still largely unclear. We recently showed that Goto–Kakizaki (GK) rats, a lean and moderate model of type 2 diabetes, have excessive cerebral neovascularisation and that these newly formed and remodelled vessels are poorly organised, poorly perfused, immature and lack pericyte support [7]. Better understanding of the regulation of cerebrovascular architecture in diabetes will identify novel targets for prevention and treatment of cerebral complications associated with the disease.

Roundabout (ROBO) family members were originally discovered as axon guidance molecules that mediate repulsive signalling mechanisms in the central nervous system [8–10]. ROBO4 is an endothelial-cell-specific ROBO protein that can bind to Slit-2. The Slit-2–ROBO4 signalling pathway regulates endothelial permeability and maintains the integrity of the vascular network by inhibiting cytokine-mediated vasculogenesis and hyperpermeability [11, 12]. Slit proteins are secreted by glial cells and other tissues [9, 13]. ROBO4 is predominantly expressed in endothelial cells, including embryonic endothelium and tumour vascular endothelium, and is structurally different from the other ROBO proteins [14, 15]. Whether and to what extent ROBO4 expression is altered in the diabetic brain vasculature is not known.

Vascular endothelial growth factor (VEGF) is a key driver of neovascularisation and vascular permeability [16–18]. We demonstrated that diabetes-induced cerebral neovascularisation is accompanied by elevated VEGF-A expression and VEGF receptor-2 (VEGFR-2) activation [7]. Furthermore, primary brain endothelial cells isolated from GK rats retained elevated VEGF-induced angiogenic properties. Studies carried out over the past decade have shown that ROBO4–Slit-2 signalling inhibits the VEGF signal [10, 11, 19, 20]. A crosstalk exists between VEGFR-2 and integrin $\alpha_v\beta_3$ such that VEGF activates β3 integrin via phosphorylation (tyrosine 747) contributing to pathological angiogenesis [21–24]. Recent

reports showed possible binding between ROBO4 and integrin [20]. Yet, little is known regarding the complex interaction between VEGF, ROBO4 and β3 integrin in diabetes.

In the present study, we tested the following hypotheses: (1) augmented VEGF signalling in diabetes decreases endothelial ROBO4 expression in the cerebral vasculature via promotion of its binding to activated β3 integrin and (2) restoration of ROBO4 expression prevents/repairs cerebral neovascularisation in diabetes.

## Methods

### Animals

Experiments were performed using Wistar and diabetic GK rats (in-house bred, derived from the Tampa colony or purchased from the Tampa colony, Taconic, Hudson, NY, USA). Since the GK model was developed from glucose-intolerant Wistar rats, this strain was used as control as previously described [7, 25, 26]. The rats were housed at the Augusta University animal care facility which is approved by the American Association for Accreditation of Laboratory Animal Care. All protocols were approved by the institutional animal care and use committee. Rats were fed standard rat chow and tap water ad libitum. Body weight and blood glucose measurements were taken biweekly. Blood glucose measurements were taken from tail-vein samples using a commercially available glucometer (Freestyle; Abbott Diabetes Care, Alameda, CA, USA). $HbA_{1c}$ was measured using A1CNow strips (Polymer Technology, Indianapolis, IN, USA). Urine albumin was measured using Chemstrip Micral stips (Roche, Indianapolis, IN, USA); results were scored as null, + (20 mg/l), ++ (50 mg/l) and +++ (100 mg/l). Body weight, blood glucose, $HbA_{1c}$ and albuminuria are presented in Table 1.

### Randomisation

Upon arrival, rats were randomised to receive either vehicle or treatment by cage. Rats were treated with a cell-permeable, selective and potent VEGFR-2 kinase inhibitor VII, SKLB1002 (Millipore, Billerica, MA, USA), at a dose of 10 mg/kg body weight, delivered daily by intraperitoneal injection for 2 weeks. For preventive studies, SLKB1002 treatment was started at 10 week of age at the onset of diabetes. For reparative studies, treatment was started 14 weeks after development of vascular disease.

### Assessment of neovascularisation

Vascularisation patterns and density were measured using the space-filling FITC–dextran (mol. wt 2,000,000; Sigma, St Louis, MO, USA) method as we recently described [27, 28]. Briefly, rats were anaesthetised and injected with FITC–dextran via the jugular vein 10 min before being killed. Brains were cut into 2 mm slices (labelled A–G, rostral to caudal; Fig. 2c). Z-stacked confocal images of 50–100 μm sections from region C (medial, where the middle cerebral artery [MCA] branches out to supply the frontal motor cortex, bregma 1 to −1) were acquired using a Zeiss 780 upright confocal microscope (Carl Zeiss MicroImaging, Thornwood, NY, USA). Regions of interest (ROI) within the cortex and striatum were based on our previous findings demonstrating the location of infarcts and haemorrhage in rats after induction of focal ischaemic stroke. All images were captured by the same operator to

ensure that the same imaging parameters were used. Analyses of the acquired images were performed by an investigator blinded to the experimental groups. Vascular volume and vascular surface area were measured using Volocity 6 software (Improvision, Lexington, MA, USA). The vascular volume represented the ratio of the volume of the vasculature to the total volume of the whole section on a stacked image and surface area was calculated as the surface area of the vasculature that was normalised to the thickness of the stacked image. Vascular density and tortuosity index were calculated using FIJI software, an image processing and analysis version of the ImageJ software (https://imagej.nih.gov/ij/index.html). Vascular density refers to the density of FITC-stained vasculature from the merged planes over the total number of planes in the section. To assess vessel tortuosity, the tortuosity index was calculated as the ratio between branch length and Euclidian distance of the branch. ROI measurement from one rat comprised a mean value of six images from either the cortical or striatal region [7].

### Immunolocalisation studies

Brain sections were blocked using 0.1% horse serum dissolved in 1% BSA in 0.3% Triton X-100 in PBS. Sections were reacted to polyclonal anti-ROBO4 antibody (Abcam, Cambridge, MA, USA). Antibodies were validated using a negative control method. Primary antibodies were specific for rat and used in 1:200 dilutions in 1% BSA in 0.3% Triton X-100 in PBS. Sections were then incubated with 1:1000 dilutions of Texas Red-conjugated goat anti-mouse or goat anti-rabbit antibodies (Invitrogen, Carlsbad, CA, USA) for 2 h. Samples were washed with PBS and imaged. ROI were imaged using a Zeiss 780 upright confocal microscope and were analysed, by a researcher blinded to grouping, for optical density using Image J software.

### Pericyte identification

Brain sections were blocked using 0.1% horse serum dissolved in 1% BSA in 0.3% Triton X-100 in PBS. Sections were reacted to rabbit polyclonal anti-platelet-derived growth factor (PDGF) receptor-β antibody (Santa Cruz, Cambridge, MA, USA). The primary antibody was specific for rat and used in 1:200 dilutions in 1% BSA in 0.3% Triton X-100 in PBS. Slides then were mounted with DAPI nuclear stain (Vector Laboratories, Burlingame, CA, USA). The pericyte nucleus was identified as a round nucleus, compared with the elliptical endothelial cell nucleus, in the vascular area and was further confirmed with PDGF receptor-β antibody (Abcam). Images of the ROI were selected as described in Fig. 2d and were acquired using a Zeiss 780 upright confocal microscope.

### ROBO4 overexpression

**In vivo experiments—***Robo4* adenovirus (3 μl of $1.85 \times 10^{12}$ viral particles/ml, Ad-*Gfp*-h*Robo4*, ADV-221472; Vector Biolabs, Philadelphia, PA, USA) was injected over 6 min via a 30-gauge needle adjacent to the MCA at stereotactic coordinates (bregma: anterior–posterior, −0.5 mm; mediolateral −1 mm; dorsoventral, −4 mm). ROBO4 overexpression was confirmed by western blot analysis and green fluorescent protein (GFP) expression 2 weeks after injection. The control group received GFP-tagged empty vector.

**In vitro experiments—**Brain microvascular endothelial cells (BMVECs) were isolated as described previously [29]. Experiments were performed using cells between passages 4 and 6. Transfection of BMVECs was performed using Amaxa Nucleofector and a kit for primary endothelial cells (Lonza, Cologne, Germany), following the manufacturer's protocol. Optimisation experiments showed that the T023 programme and 300 ng of ROBO4 plasmid (Qiagen, Valencia, CA, USA) gave the maximum transfection efficacy of 85% for BMVECs. Cells suspended in a nucleofection mixture with the ROBO4 plasmid and pmax-GFP (Lonza, Cologne, Germany) were electroporated and left in complete medium for 36 h to recover before experiments were performed. Control cells received pmax-GFP plasmid only.

## Gene silencing

BMVECs were transfected with either scrambled, *Robo4* small interfering RNA (siRNA) or β3 integrin (*Itgb3*) siRNA (Santa Cruz) using Amaxa Nucleofector kit, following the manufacturer's protocol (Lonza). Optimisation experiments showed that the T005 programme and 300 nmol/l of siRNA gave the maximum transfection efficacy (80–90%) and this was confirmed by western blotting (40–50% reduction). Cells suspended in a nucleofection mixture with the siRNA and pmax-GFP were electroporated and left to recover in complete medium for 24 h. Experiments were performed three times in duplicate within 72 h of transfection.

## Cell migration, tube formation and permeability assays

The wound healing and tube formation assays were performed as described previously [29]. Briefly, a monolayer of cells was scratched and imaged at zero time and after 18 h. Images were acquired using an Axiovert 200 microscope (Carl Zeiss). Images were analysed for the percentage of migration. For the tube formation assay, equal numbers of cells were grown in 3D Matrigel overnight and imaged after 18 h. Images were analysed for mean tube count per field. For permeability assay, BMVECs were cultured in Transwell plates (Corning Life Sciences, Acton, MA, USA) for 24 h in complete medium and then in serum-free medium for an additional 24 h. the confluent monolayer of BMVECs in the upper chamber of the Transwells was treated with FITC–dextran (1 mg/ml, mol. wt 150,000; Sigma). The fluorescence intensity, equivalent to the relative amount of FITC–dextran in the lower chambers of the Transwells, was measured over a 30 min period and determined using a Biotek Spectrometer (Biotek Instruments, Winooski, VT, USA) (excitation wavelength, 485 nm; emission wavelength, 530 nm). Experiments were performed three times in duplicates.

## Immunoprecipitation and western blot analysis

Brain homogenate (30–50 μg) in modified RIPA buffer (Millipore) was boiled with Laemmli sample buffer, separated on a 4–15% gradient SDS-polyacrylamide gel by electrophoresis, transferred to a nitrocellulose membrane and stained with a specific antibody. All primary antibodies were rat specific: anti-ROBO4 and anti-β3 integrin antibodies were purchased from Abcam (rabbit polyclonal, 1:500) and anti-phospho β3 integrin, -actin, -VEGFR-2 and -phospho-VEGFR-2 were from Millipore (mouse, monoclonal, 1:500). For immunoprecipitation, equal loads of brain homogenates were treated with anti-β3 integrin antibodies overnight and immunoblotted with anti-ROBO4 antibody. Relative optical

densities of immunoreactivity were determined by Alpha-View densitometry software (version 3.4.0; Alpha Innotech, ProteinSimple, San Jose, CA, USA).

### Inclusion and exclusion criteria

All data points were included in the data analyses.

### Statistical analysis

Statistical significance for all analyses was assessed at an α level of 0.05 using SAS version 9.3 (SAS Institute, Cary, NC, USA). Comparisons were made between vehicle and VEGF antagonist (SKLB1002) or *Robo4* adenovirus-treated GK rats using two-sample *t* tests. Comparisons between measurements made on the control and treated sides of the brain were made using a paired *t* test. One-way ANOVA was used to compare groups in Figs 2a–c, 4a–d. A Tukey's adjustment for multiple comparisons was used for all post hoc mean comparisons for significant effects from all analyses. Results are presented by means ± SEM.

## Results

### Diabetes decreases the expression of ROBO4

ROBO4 expression was significantly lower in the cerebral vasculature of diabetic GK rats compared with control non-diabetic Wistar rats (Fig. 1a). This was confirmed by measuring ROBO4 protein levels in BMVECs isolated from diabetic and control rats (Fig. 1b).

### ROBO4 overexpression restores augmented VEGF-induced angiogenic signal

Silencing *Robo4* expression by approximately 40% (data not shown) in BMVECs isolated from control Wistar rats increased the cells' angiogenic properties, as shown by increased cell migration and tube formation compared with BMVECs transfected with scrambled siRNA (Fig. 2a). Consistent with previous findings, BMVECs isolated from diabetic rats displayed augmented pro-angiogenic behaviour such as increased migration and tube formation [7]. Overexpression of ROBO4 (80–90% transfection efficiency, data not shown), significantly reduced migration, tube formation and cell Transwell permeability in BMVECs isolated from diabetic rats compared with pmax-GFP transfected diabetic rats (Fig. 2a, b). In vivo, ROBO4 was overexpressed in the brains of the diabetic GK rats using an adenovirus construct that contains GFP-tagged ROBO4. Two weeks after unilateral stereotactic injection of the adenovirus, the ipsilateral vasculature was compared with the vasculature in the contralateral hemisphere of the brain (Fig. 2c); a 50% increase in expression was confirmed using immunoblotting. In vivo overexpression of ROBO4 significantly reduced all indices of neovascularisation (Fig. 2d). Vascularisation in control rats that had received GFP-tagged empty vector was comparable with the contralateral hemisphere in rats that had received unilateral GFP-tagged ROBO4, indicating that the injection procedure did not affect the vascularisation response.

### ROBO4 overexpression increases vascular stability

We examined the vascular pericyte coverage as an index of vascular maturity and stability after overexpression of ROBO4 in the cerebral vasculature. Pericytes were quantified using nuclear morphology with nuclear DAPI stain (Fig. 3a) and confirmed with immunostaining using anti-PDGF receptor-β antibody (Fig. 3b). Overexpression of ROBO4 significantly increased the pericyte-to-endothelial cell ratio in the cerebral vasculature.

### VEGFR-2 inhibitor SKLB1002 increases ROBO4 availability

A dose-finding study showed that treatment of diabetic GK rats with 10 mg/kg SKLB1002 each day for 2 weeks significantly inhibited VEGFR-2 phosphorylation (Fig. 4a). Treatment with SLKB1002 (10 and 15 mg/kg per day for 2 weeks) significantly increased ROBO4 expression in brain homogenates (Fig. 4b). VEGFR-2 inhibition or ROBO4 overexpression caused significant reduction of VEGF-induced activation and phosphorylation of β3 integrin (Fig. 4c). In addition, immunoprecipitation studies showed that VEGFR-2 inhibition or ROBO4 overexpression significantly decreased the ROBO4–β3 integrin interaction (Fig. 4d). In parallel, silencing the β3 integrin gene using siRNA significantly reduced the augmented angiogenic properties of BMVECs isolated from diabetic rats (Fig. 4e).

### Inhibition of VEGF angiogenic signalling with SKLB1002 prevents/repairs cerebral neovascularisation in diabetes

Early treatment of diabetic GK rats with VEGFR-2 inhibitor for 2 weeks significantly prevented cerebral neovascularisation as shown by reduction in cerebrovascular volume, surface area, vascular density and tortuosity (Fig. 5b). To determine the therapeutic potential of VEGF-R2 inhibition, 14-week-old diabetic GK rats with established vascular disease were treated with the VEGFR-2 inhibitor for 2 weeks. SLKB1002 treatment significantly reduced all neovascularisation indices in the cortex and striatum (Fig. 5c).

## Discussion

The present study provides novel evidence that increased VEGF signalling in cerebral vessels in diabetes decreases the expression and availability of ROBO4 via binding with VEGF-activated β3 integrin. In vitro and in vivo overexpression of ROBO4 reduces the augmented VEGF-induced angiogenic signal and decreases cerebral neovascularisation in diabetes. Inhibition of the VEGF angiogenic signal using SKLB1002, a selective VEGFR-2 antagonist, decreases ROBO4–β3 integrin interaction, increases the expression and availability of ROBO4 and prevents/repairs cerebral neovascularisation in diabetes. (Fig. 6)

We previously showed that diabetes causes cerebral neovascularisation in different models of diabetes including GK rats and *db*/*db* mice [25]. Similar findings were made in other rat models of diabetes such as the high-fat-diet/low-dose streptozotocin model (data not shown). GK rats, a lean and moderate model of type 2 diabetes, develop remodelled vessels that are poorly organised, poorly perfused, leaky and lack pericyte support. These changes are associated with increased VEGF signal [7]. Better understanding of the regulation of cerebral neovascularisation in diabetes is necessary to identify preventive and therapeutic strategies aimed against cerebral complications.

ROBO4 is an endothelial cell-specific ROBO trans-membrane receptor that regulates endothelial permeability and maintains the integrity of the vascular network. Slit-2 is the main ligand and ROBO4–Slit-2 inhibits cytokine-mediated vasculogenesis and hyperpermeability [11, 12]. We and others showed that ROBO4 is endogenously expressed in BMVECs [30]. This study provided evidence that diabetic GK rats showed a significant reduction in ROBO4 expression in cerebral vessels and in isolated BMVECs.

In the present study, we tested the hypothesis that increased VEGF signalling in diabetes decreases the function and availability of ROBO4, leading to increased cerebral neovascularisation. The use of anti-VEGF treatments in diabetes is limited to diabetic retinopathy in which local application of the drug is preferred. However, pharmacological VEGF inhibition has been used successfully to prevent tumour angiogenesis and growth. VEGF is a well-known survival factor acting through multiple receptors. Unfortunately, while the treatment was effective in preventing or reducing tumour growth, many patients suffered from adverse effects including increases in blood pressure and kidney failure [31]. Therefore, it is essential to block the downstream angiogenic signal, mediated mainly via VEGF-R2, while maintaining other protective effects. SKLB1002, a cell-permeable potent VEGFR-2 selective inhibitor, was chosen for its reduced or little activity against 16 other kinases [32]. SKLB1002 suppresses tumour growth in mice via inhibition of angiogenesis [33]. To minimise possible systemic side effects while antagonising VEGF, a dose-finding study identified a small dose that is tenfold less that that used in tumour studies and sufficiently suppresses VEGFR-2 activation without any effect on blood pressure and proteinuria. SKLB1002 treatment prevented/reversed diabetes-induced neovascularisation that was associated with increased ROBO4 expression and function. Our novel studies support our hypothesis and expand our knowledge regarding the use of low-dose anti-VEGF treatments in the prevention of diabetes-induced cerebrovascular complications. We used additional molecular gain- and loss-of-function approaches to further test our hypothesis. ROBO4 was overexpressed either locally in the striatum in vivo or in BMVECs in vitro. ROBO4 overexpression decreased all indices of neovascularisation at the injection site and increased vessel stability and maturation, as shown by increased pericyte coverage. In cells, ROBO4 overexpression decreased migration and improved barrier function, as indicated by reduced permeability. Conversely, knockdown of ROBO4 in control cells resulted in an angiogenic phenotype like that observed in cells isolated from diabetic rats. Our findings are in agreement with those of recent studies wherein ROBO4 signalling was found to promote vascular stability via modulation of VEGF signalling [11, 34–37]. Similar to our finding, Cai et al showed that knocking down of ROBO4 increases endothelial permeability, decreases trans-endothelial electrical resistance values, downregulates expression of the endothelial tight junction proteins and increases matrix metalloproteinase-9 (MMP-9) activity [38]. The same group also showed that ROBO4 suppresses endothelial cell proliferation, migration and tube formation in vitro by inhibiting VEGR2-mediated phosphoinositide 3-kinase (PI3K)/Akt and focal adhesion kinase (FAK) signalling pathways [30]. Our study expands these findings in the context of diabetes and suggest that restoration of ROBO4 expression prevents neovascularisation and improves cerebrovascular integrity in diabetes.

Studies demonstrated that VEGF activates β3 integrin via phosphorylation at tyrosine 747 [22, 23, 39–42]. Furthermore, one study also showed that ROBO4 binds to integrin, which

causes inactivation of ROBO4–Slit-2 signalling and promotes vascular hyperpermeability [20]. To investigate whether this complex interaction is the underlying molecular mechanism by which VEGF signalling reduces ROBO4 availability in diabetes, we examined whether ROBO4 and β3 integrin interact in our model. Both VEGF inhibition and ROBO4 overexpression decreased β3 integrin activation as well as reducing the interaction between ROBO4 and β3 integrin, suggesting a feedback loop between ROBO4 and VEGF signalling.

Based on our previous studies, we believe that diabetes-induced cerebral neovascularisation is a pathological process. We have shown that these vessels are leaky, lack pericyte coverage and have increased MMP-2, -3 and -9 activity [7, 43]. We reported vascular dysfunction and hypoxia in the brain before stroke [44]. Moreover, animals show cognitive deficits even before stroke and these newly formed vessels bleed upon ischaemic insult, worsening stroke outcomes [7, 25, 26, 43, 44]. For all these reasons, we believe that these vessels are dysfunctional. However, this process may also be a homeostatic response to overcome cerebral hypoxia.

There are limitations to this study. First, we focused on ROBO4 and did not address the role of Slit2–ROBO1 signalling, which has been shown to be pro-angiogenic [45]. Second, the in vivo overexpression approach is not specific for endothelial cells. However, these limitations do not affect the significance of our study, which used a combination of in vivo and in vitro techniques coupled with molecular and pharmacological gain- or loss-of-function approaches and provided evidence that restoration of ROBO4 expression and inhibition of VEGF signalling prevent cerebral neovascularisation in diabetes. Future studies focusing on the functional outcomes of cerebral ROBO4 restoration may help us determine whether these vascular changes are pathological. For example, improvement of cognitive function or attenuation of bleeding after stroke when neovascularisation is prevented by ROBO4 overexpression or VEGF inhibition would provide additional support for this concept and would also identify the therapeutic potential of ROBO4 targeting in diabetes.

## Acknowledgments

**Funding**

AE is a Research Career Scientist at the Charlie Norwood Veterans Affairs Medical Center in Augusta, Georgia. This work was supported in part by a Veterans Affairs (VA) Merit Award (BX000347), VA Research Career Scientist Award and National Institutes of Health (NIH) award (R01NS083559) to AE and an American Heart Association Postdoctoral Fellowship (14POST19580004) and Scientist Development Grant (16SDG30270013) to MA. The contents do not represent the views of the Department of Veterans Affairs or the US Government.

## Abbreviations

| | |
|---|---|
| **BMVEC** | Brain microvascular endothelial cell |
| **GFP** | Green fluorescent protein |
| **GK** | Goto–Kakizaki |
| **MCA** | Middle cerebral artery |
| **MMP-9** | Matrix metalloproteinase-9 |

| | |
|---|---|
| **PDGF** | Platelet-derived growth factor |
| **ROBO** | Roundabout |
| **ROI** | Region(s) of interest |
| **siRNA** | Small interfering ribonucleic acids |
| **VEGFR-2** | VEGF receptor-2 |
| **VEGF** | Vascular endothelial growth factor |

## References


1. Ergul A, Li W, Elgebaly MM, Bruno A, Fagan SC. Hyperglycemia, diabetes and stroke: focus on the cerebrovasculature. Vascul Pharmacol. 2009; 51:44–49. [PubMed: 19258053]
2. Mogi M, Horiuchi M. Neurovascular coupling in cognitive impairment associated with diabetes mellitus. Circ J. 2011; 75:1042–1048. [PubMed: 21441696]
3. Giacco F, Brownlee M. Oxidative stress and diabetic complications. Circ Res. 2010; 107:1058–1070. [PubMed: 21030723]
4. Snell-Bergeon JK, Wadwa RP. Hypoglycemia, diabetes, and cardiovascular disease. Diabetes Technol Ther. 2012; 14(Suppl 1):S51–S58. [PubMed: 22650225]
5. Dalkara T, Gursoy-Ozdemir Y, Yemisci M. Brain microvascular pericytes in health and disease. Acta Neuropathol. 2011; 122:1–9. [PubMed: 21656168]
6. Whitmire W, Al-Gayyar MM, Abdelsaid M, Yousufzai BK, El-Remessy AB. Alteration of growth factors and neuronal death in diabetic retinopathy: what we have learned so far. Mol Vis. 2011; 17:300–308. [PubMed: 21293735]
7. Prakash R, Somanath PR, El-Remessy AB, et al. Enhanced cerebral but not peripheral angiogenesis in the Goto-Kakizaki model of type 2 diabetes involves VEGF and peroxynitrite signaling. Diabetes. 2012; 61:1533–1542. [PubMed: 22403298]
8. Brose K, Bland KS, Wang KH, et al. Slit proteins bind Robo receptors and have an evolutionarily conserved role in repulsive axon guidance. Cell. 1999; 96:795–806. [PubMed: 10102268]
9. Kidd T, Bland KS, Goodman CS. Slit is the midline repellent for the robo receptor in Drosophila. Cell. 1999; 96:785–794. [PubMed: 10102267]
10. Andrews W, Barber M, Hernadez-Miranda LR, et al. The role of Slit-Robo signaling in the generation, migration and morphological differentiation of cortical interneurons. Dev Biol. 2008; 313:648–658. [PubMed: 18054781]
11. Jones CA, London NR, Chen H, et al. Robo4 stabilizes the vascular network by inhibiting pathologic angiogenesis and endothelial hyperpermeability. Nat Med. 2008; 14:448–453. [PubMed: 18345009]
12. London NR, Zhu W, Bozza FA, et al. Targeting Robo4-dependent Slit signaling to survive the cytokine storm in sepsis and influenza. Sci Transl Med. 2010; 2:23ra19.
13. Rajagopalan S, Nicolas E, Vivancos V, Berger J, Dickson BJ. Crossing the midline: roles and regulation of Robo receptors. Neuron. 2000; 28:767–777. [PubMed: 11163265]
14. Legg JA, Herbert JM, Clissold P, Bicknell R. Slits and Roundabouts in cancer, tumour angiogenesis and endothelial cell migration. Angiogenesis. 2008; 11:13–21. [PubMed: 18264786]
15. Huang L, Yu W, Li X, et al. Expression of Robo4 in the fibrovascular membranes from patients with proliferative diabetic retinopathy and its role in RF/6A and RPE cells. Mol Vis. 2009; 15:1057–1069. [PubMed: 19495426]
16. Chung AS, Ferrara N. Developmental and pathological angiogenesis. Annu Rev Cell Dev Biol. 2011; 27:563–584. [PubMed: 21756109]
17. Abdelsaid MA, El-Remessy AB. S-glutathionylation of LMW-PTP regulates VEGF-mediated FAK activation and endothelial cell migration. J Cell Sci. 2012; 125:4751–4760. [PubMed: 22854047]

18. Kajdaniuk D, Marek B, Foltyn W, Kos-Kudla B. Vascular endothelial growth factor (VEGF) - part 1: in physiology and pathophysiology. Endokrynol Pol. 2011; 62:444–455. [PubMed: 22069106]
19. Koch AW, Mathivet T, Larrivee B, et al. Robo4 maintains vessel integrity and inhibits angiogenesis by interacting with UNC5B. Dev Cell. 2011; 20:33–46. [PubMed: 21238923]
20. Zhang X, Yu J, Kuzontkoski PM, Zhu W, Li DY, Groopman JE. Slit2/Robo4 signaling modulates HIV-1 gp120-induced lymphatic hyperpermeability. PLoS Pathog. 2012; 8:e1002461. [PubMed: 22241990]
21. De S, Razorenova O, McCabe NP, O'Toole T, Qin J, Byzova TV. VEGF-integrin interplay controls tumor growth and vascularization. Proc Natl Acad Sci U S A. 2005; 102:7589–7594. [PubMed: 15897451]
22. Di Q, Cheng Z, Kim W, et al. Impaired cross-activation of beta3 integrin and VEGFR-2 on endothelial progenitor cells with aging decreases angiogenesis in response to hypoxia. Int J Cardiol. 2013; 168:2167–2176. [PubMed: 23452889]
23. West XZ, Meller N, Malinin NL, et al. Integrin beta3 crosstalk with VEGFR accommodating tyrosine phosphorylation as a regulatory switch. PLoS One. 2012; 7:e31071. [PubMed: 22363548]
24. Papo N, Silverman AP, Lahti JL, Cochran JR. Antagonistic VEGF variants engineered to simultaneously bind to and inhibit VEGFR2 and $\alpha_v\beta_3$ integrin. Proc Natl Acad Sci U S A. 2011; 108:14067–14072. [PubMed: 21825147]
25. Prakash R, Johnson M, Fagan SC, Ergul A. Cerebral neovascularization and remodeling patterns in two different models of type 2 diabetes. PLoS One. 2013; 8:e56264. [PubMed: 23441170]
26. Prakash R, Li W, Qu Z, Johnson MA, Fagan SC, Ergul A. Vascularization pattern after ischemic stroke is different in control versus diabetic rats: relevance to stroke recovery. Stroke. 2013; 44:2875–2882. [PubMed: 23920018]
27. Abdelsaid M, Kaczmarek J, Coucha M, Ergul A. Dual endothelin receptor antagonism with bosentan reverses established vascular remodeling and dysfunctional angiogenesis in diabetic rats: Relevance to glycemic control. Life Sci. 2014; 118:268–273. [PubMed: 24447630]
28. Abdelsaid M, Ma H, Coucha M, Ergul A. Late dual endothelin receptor blockade with bosentan restores impaired cerebrovascular function in diabetes. Life Sci. 2014; 118:263–267. [PubMed: 24434796]
29. Abdelsaid M, Prakash R, Li W, et al. Metformin treatment in the period after stroke prevents nitrative stress and restores angiogenic signaling in the brain in diabetes. Diabetes. 2015; 64:1804–1817. [PubMed: 25524911]
30. Cai H, Xue Y, Li Z, et al. Roundabout4 suppresses glioma-induced endothelial cell proliferation, migration and tube formation in vitro by inhibiting VEGR2-mediated PI3K/AKT and FAK signaling pathways. Cell Physiol Biochem. 2015; 35:1689–1705. [PubMed: 25833462]
31. Kamba T, McDonald DM. Mechanisms of adverse effects of anti-VEGF therapy for cancer. Br J Cancer. 2007; 96:1788–1795. [PubMed: 17519900]
32. Zhang S, Cao Z, Tian H, et al. SKLB1002, a novel potent inhibitor of VEGF receptor 2 signaling, inhibits angiogenesis and tumor growth in vivo. Clin Cancer Res. 2011; 17:4439–4450. [PubMed: 21622720]
33. Shen G, Li Y, Du T, et al. SKLB1002, a novel inhibitor of VEGF receptor 2 signaling, induces vascular normalization to improve systemically administered chemotherapy efficacy. Neoplasma. 2012; 59:486–493. [PubMed: 22668017]
34. Jones CA, Nishiya N, London NR, et al. Slit2-Robo4 signalling promotes vascular stability by blocking Arf6 activity. Nat Cell Biol. 2009; 11:1325–1331. [PubMed: 19855388]
35. Marlow R, Binnewies M, Sorensen LK, et al. Vascular Robo4 restricts proangiogenic VEGF signaling in breast. Proc Natl Acad Sci U S A. 2010; 107:10520–10525. [PubMed: 20498081]
36. Tian R, Liu ZX, Zhang H, et al. Investigation of the regulation of roundabout4 (Robo4) by hypoxia-inducible factor-1α in Microvascular Endothelial Cells. Invest Ophthalmol Vis Sci. 2015; 56:2586–2594. [PubMed: 26066603]
37. Xie J, Liu X, Li Y, Liu Y, Su G. Validation of RT-qPCR reference genes and determination of Robo4 expression levels in human retinal endothelial cells under hypoxia and/or hyperglycemia. Gene. 2016; 585:135–142. [PubMed: 27041242]

38. Cai H, Liu W, Xue Y, et al. Roundabout 4 regulates blood-tumor barrier permeability through the modulation of ZO-1, Occludin, and Claudin-5 expression. J Neuropathol Exp Neurol. 2015; 74:25–37. [PubMed: 25470344]

39. Somanath PR, Malinin NL, Byzova TV. Cooperation between integrin $\alpha_V\beta_3$ and VEGFR2 in angiogenesis. Angiogenesis. 2009; 12:177–185. [PubMed: 19267251]

40. Robinson SD, Hodivala-Dilke KM. The role of β3-integrins in tumor angiogenesis: context is everything. Curr Opin Cell Biol. 2011; 23:630–637. [PubMed: 21565482]

41. Byzova TV, Goldman CK, Pampori N, et al. A mechanism for modulation of cellular responses to VEGF: activation of the integrins. Mol Cell. 2000; 6:851–860. [PubMed: 11090623]

42. Blystone SD, Williams MP, Slater SE, Brown EJ. Requirement of integrin β3 tyrosine 747 for β3 tyrosine phosphorylation and regulation of $\alpha_V\beta_3$ avidity. J Biol Chem. 1997; 272:28757–28761. [PubMed: 9353346]

43. Hafez S, Abdelsaid M, El-Shafey S, Johnson MH, Fagan SC, Ergul A. Matrix metalloprotease 3 exacerbates hemorrhagic transformation and worsens functional outcomes in hyperglycemic stroke. Stroke. 2016; 47:843–851. [PubMed: 26839355]

44. Kelly-Cobbs AI, Prakash R, Li W, et al. Targets of vascular protection in acute ischemic stroke differ in type 2 diabetes. Am J Physiol Heart Circ Physiol. 2013; 304:H806–H815. [PubMed: 23335797]

45. Li S, Huang L, Sun Y, et al. Slit2 promotes angiogenic activity via the Robo1-VEGFR2-ERK1/2 pathway in both in vivo and in vitro studies. Invest Ophthalmol Vis Sci. 2015; 56:5210–5217. [PubMed: 26244297]

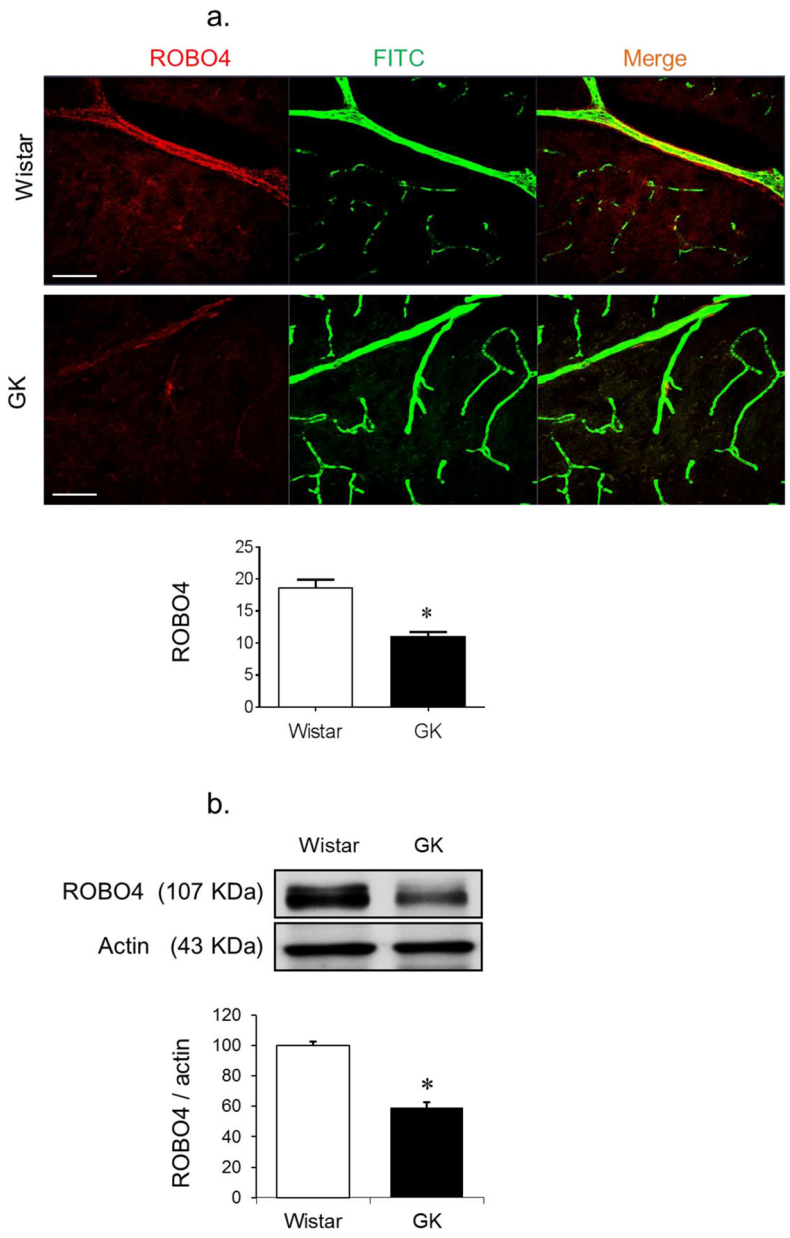


**Fig. 1.**

Diabetes decreases the expression of ROBO4 in cerebral vasculature. Diabetic GK rats were injected with FITC–dextran via the jugular vein. Brain sections were reacted with anti-ROBO4 antibody. (**a**) Co-localised ROBO4 (red) on FITC-filled cerebral vasculature (green) was compared between diabetic GK rats and control Wistar rats. Diabetic GK rats showed decreased ROBO4 expression ($n$=4 or 5, *$p$<0.05 vs Wistar). (**b**) Western blot of BMVECs isolated from control and diabetic rats, showing a significant reduction in ROBO4 expression in diabetes ($n$=3 or 4, *$p$<0.05 vs Wistar). Scale bars, 10 μm

a.

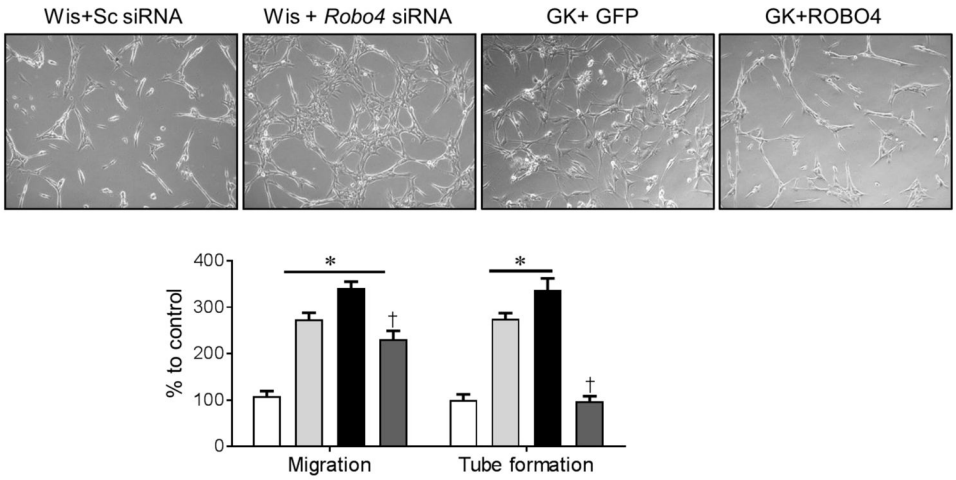


b.

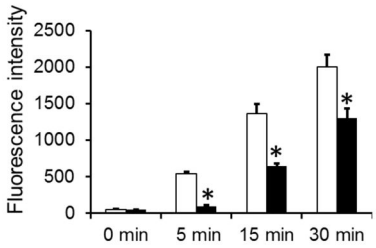

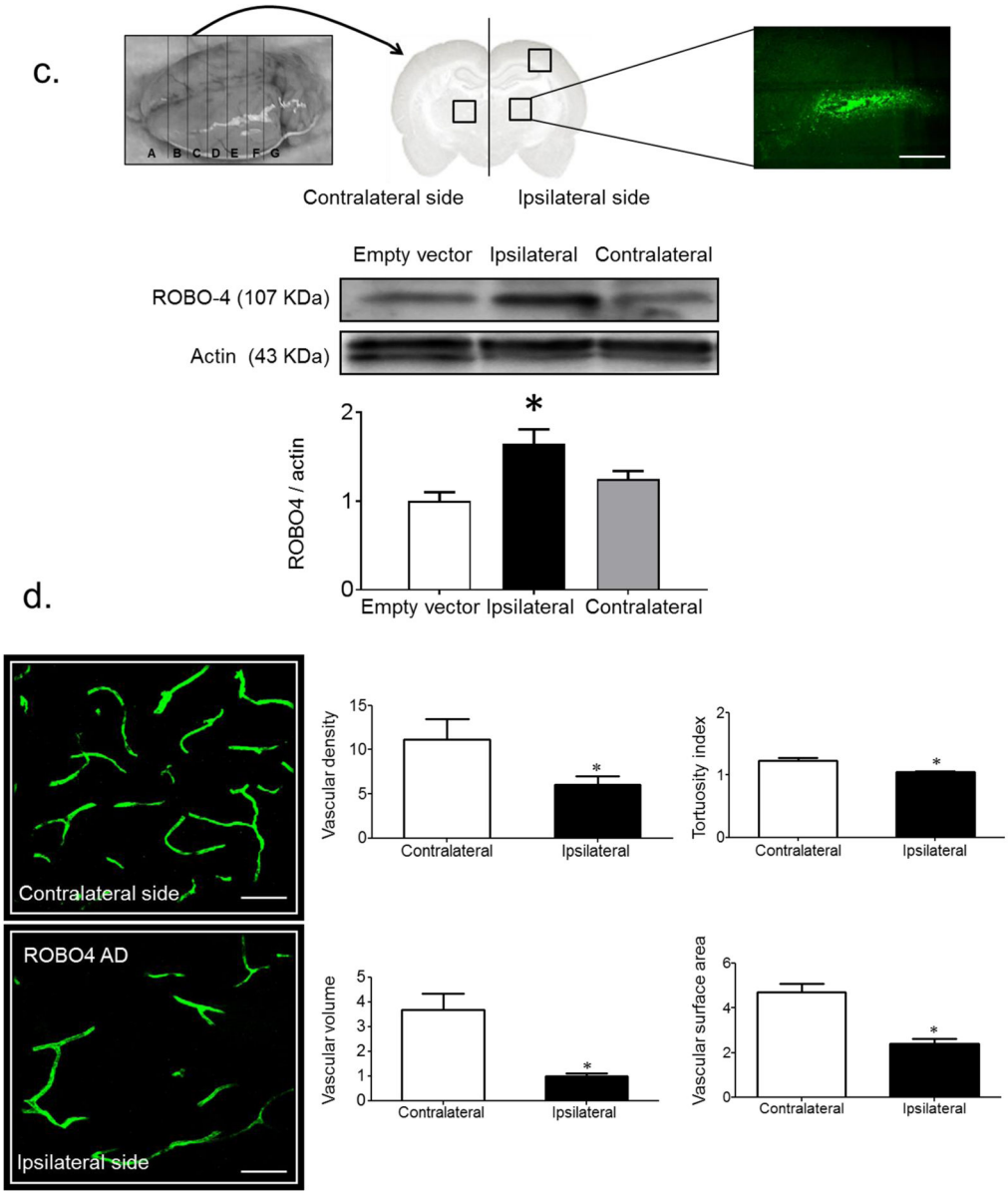


**Fig. 2.**

ROBO4 regulates VEGF-induced angiogenic signal. (**a**) Silencing *Robo4* in BMVECs isolated from control Wistar rats (Wis, light grey bars) resulted in a significant increase in migration and tube formation compared with cells transfected with scrambled (Sc) siRNA (white bars). BMVECs isolated from diabetic GK rats (black bars) showed significant increases in migration and tube formation. Overexpression of ROBO4 in diabetic BMVECs (dark grey bars) significantly decreased endothelial cell migration and tube formation ($n$=3 in duplicate, *$p$<0.05 vs Wistar+Sc siRNA, $^{\dagger}p$<0.05 vs GK+GFP). (**b**) Transwell permeability assay showed that overexpression of ROBO4 (black bars) significantly decreased BMVEC permeability in diabetes compared with control ($n$=3 in duplicate, $^{\dagger}p$<0.05 vs GK+GFP). (**c**) Representative image of brain and adenovirus stereotactic injection site. ROBO4 was overexpressed by 50% compared with empty vector

control. ($n$=3, *$p$<0.05 vs empty vector). Scale bar, 10 μm. (**d**) Representative image and quantification of neovascularisation indices after ROBO4 overexpression. ROBO4 overexpression (*Robo4* AD) significantly reduced all neovascularisation indices ($n$=4, *$p$<0.05 vs contralateral side). Scale bars, 50 μm

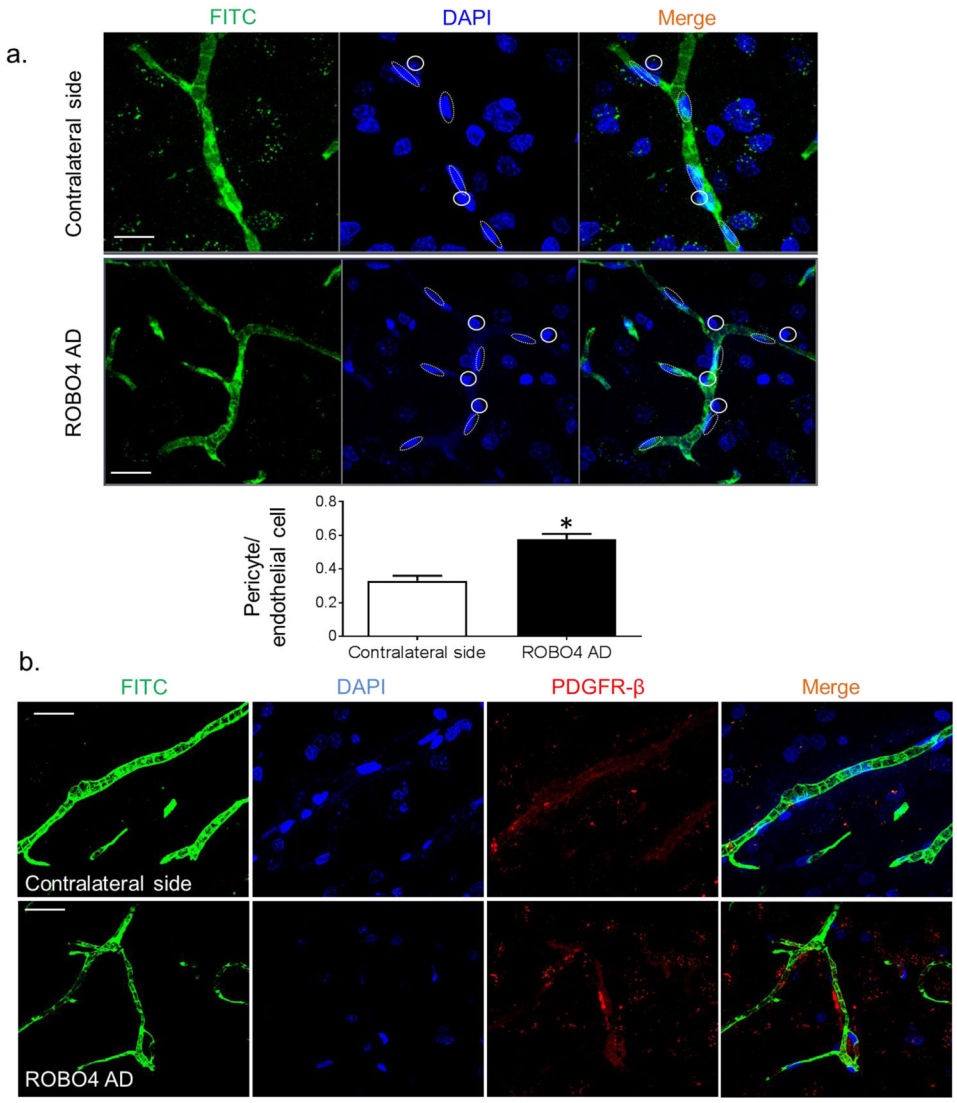


**Fig. 3.**

ROBO4 overexpression increases vascular stability. (**a**) Nuclear morphology was used to assess the pericyte-to-endothelial cell ratio. Dotted lines represent the elliptical endothelial cells nuclei and solid circles represent pericytes nuclei. Overexpression of ROBO4 (*Robo4* AD) significantly increased this ratio in the cerebral vasculature ($n$=4, *$p$<0.05 vs contralateral side). Scale bars, 10 μm. (**b**) Representative images of brain sections showing FITC-filled vessels (green), nuclear stain (DAPI, blue), pericyte marker, PDGF receptor-β antibody (red) and merged images. Scale bars, 10 μm

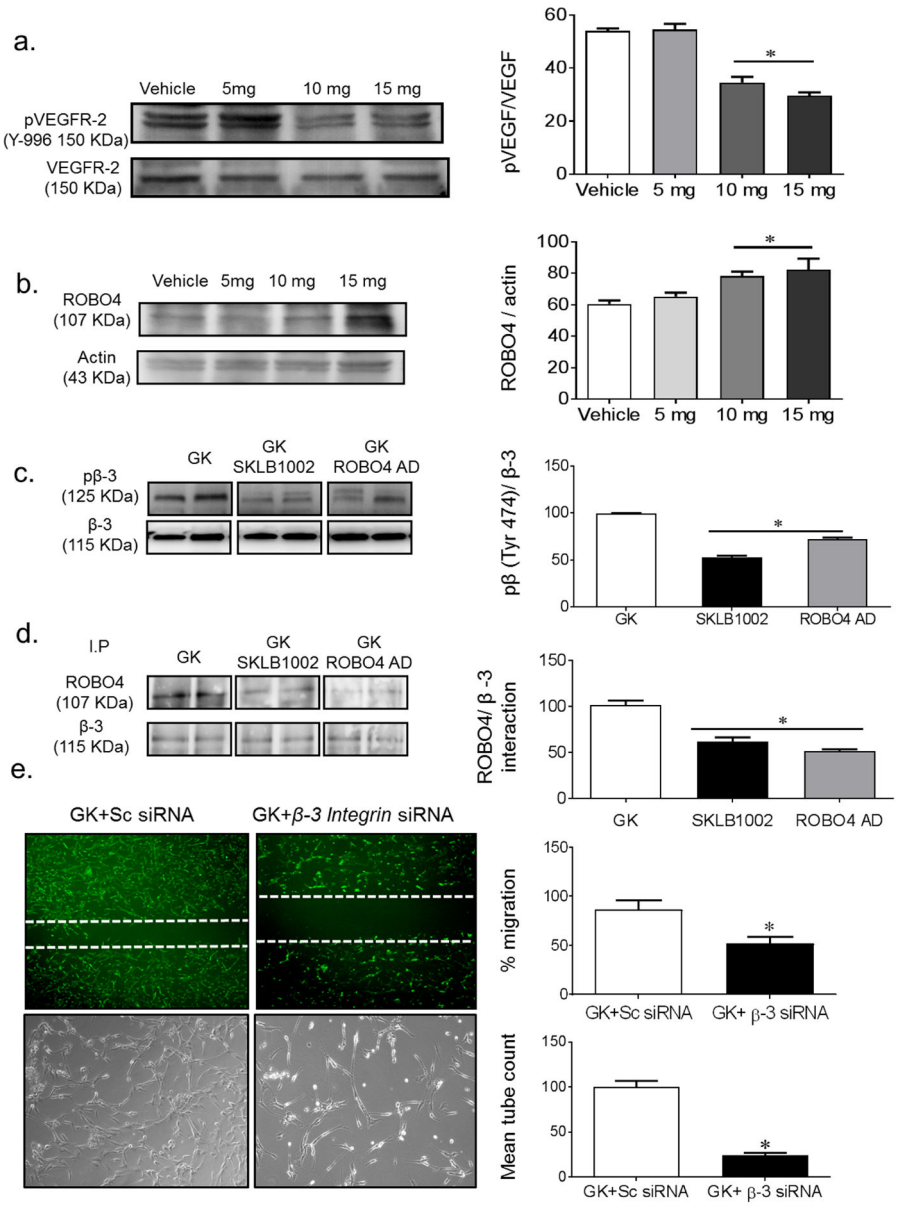


**Fig. 4.**

VEGFR-2 inhibitor, SKLB1002, increases ROBO4 availability. Diabetic GK rats were treated with vehicle or SLKB1002 (5, 10 or 15 mg/kg per day i.p.) for 2 weeks. (**a**) Western blot analysis of VEGFR-2 activation. GK rats treated with SLKB1002 showed significant decrease in VEGFR-2 phosphorylation compared with control vehicle-treated rats ($n$=3, *$p$<0.05 vs vehicle). (**b**) Western blot analysis of ROBO4 expression in GK rats treated with SLKB1002 showed increased expression of ROBO4 ($n$=3 or 4, *$p$<0.05 vs vehicle). (**c**) Western blot analysis of VEGF-induced phosphorylation of β3 integrin (β-3). Treatment with SLKB1002 or ROBO4 overexpression (ROBO4 AD) significantly reduced VEGF-induced phosphorylation of β3 integrin in GK rats. ($n$=3 or 4, *$p$<0.05 vs GK). (**d**) Immunoprecipitation (IP) of brain homogenate from GK rats treated with SKLB1002 or overexpressing ROBO4. Both treatments significantly decreased the ROBO4–β3 integrin

interaction and binding in GK brain homogenate ($n$=3 or 4, *$p$<0.05 vs GK). (**e**) Representative images and quantification of cell migration and tube formation. Dashed white lines represent migration after 18 h. Silencing the β3 integrin gene significantly decreased cellular tube formation and migration in BMVECs isolated from diabetic GK rats compared with GK BMVECs treated with scrambled siRNA (Sc siRNA) ($n$=3 in duplicate, *$p$<0.05 vs GK+Sc siRNA)

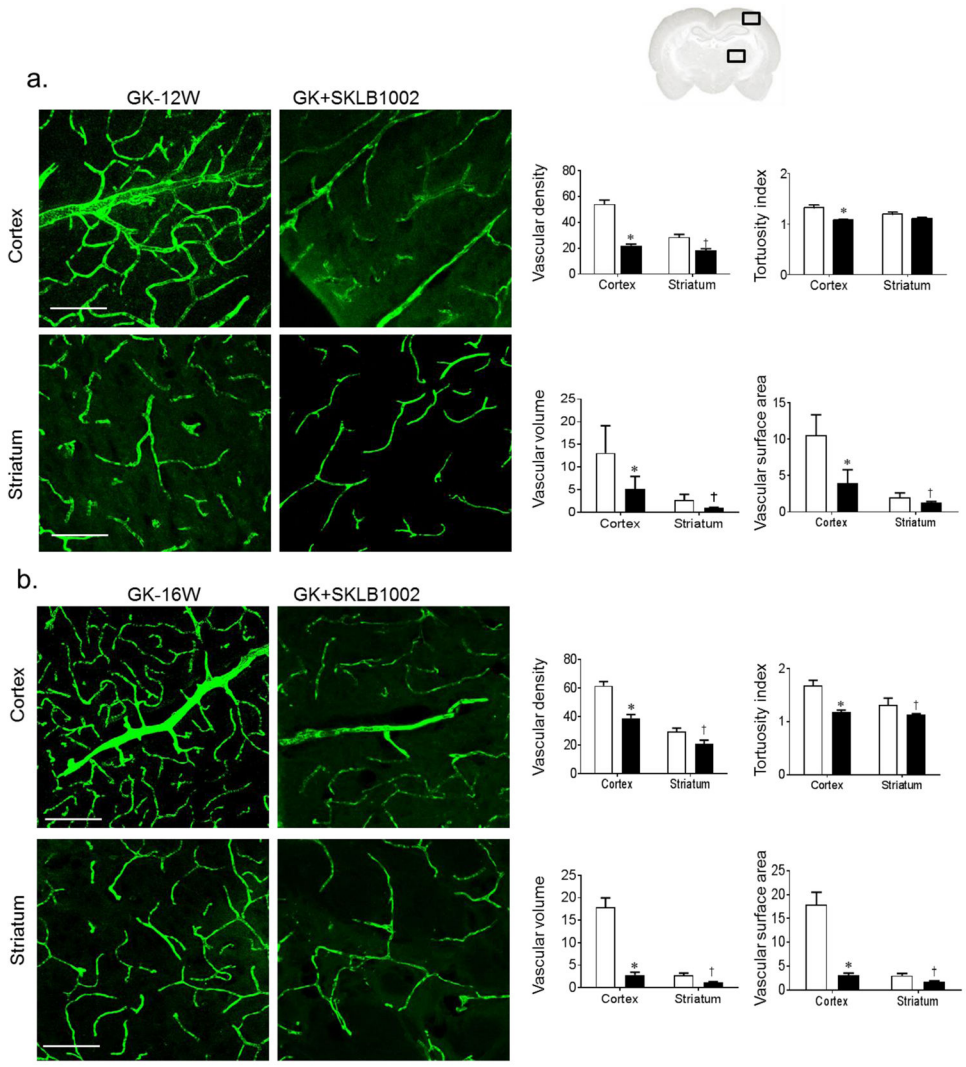


**Fig. 5.**

Inhibition of VEGF angiogenic signalling with SKLB1002 prevents/repairs cerebral neovascularisation in diabetes. (**a**) Representation of the ROI locations in the brain (cortex and striatum) (**b**) Representative images of cerebral vasculature and quantification of cerebral neovascularisation indices in 10-week-old GK rats. GK rats were treated with vehicle or the VEGFR-2 inhibitor SLKB1002 (10 mg/kg per day i.p.) for 2 weeks. SLKB1002 significantly decreased neovascularisation indices ($n$=5 or 6, *$p$<0.05 vs GK-vehicle cortex, $^{\dagger}p$<0.05 vs GK-vehicle striatum). (**b**) In 14-week-old GK rats with established neovascularisation, treatment with SLKB1002 (10 mg/kg per day i.p.) for 2 weeks significantly decreased all neovascularisation indices ($n$=5 or 6, *$p$<0.05 vs GK-vehicle cortex, $^{\dagger}p$<0.05 vs GK-vehicle striatum). Scale bars, 50 μm. White bars, GK rats; black bars, SLKB1002-treated GK rats

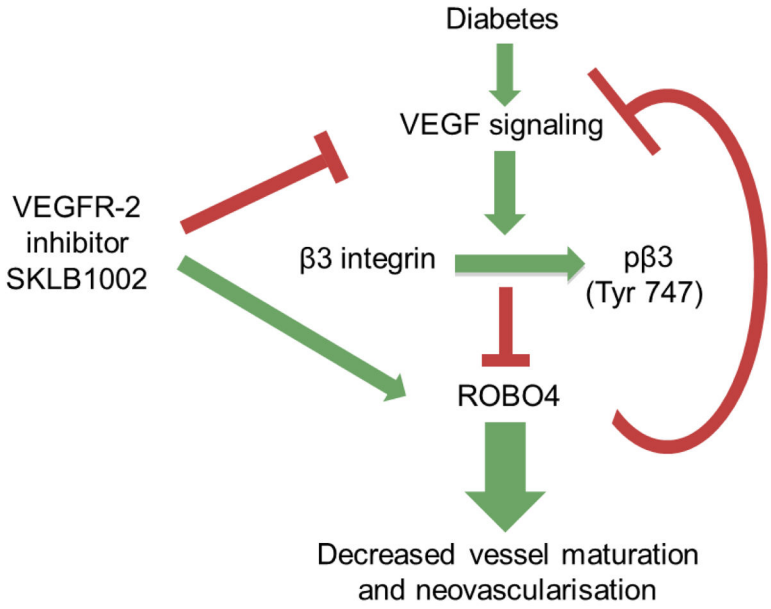


**Fig. 6.**

Increased VEGF signalling in cerebral vessels in diabetes decreases the expression and availability of ROBO4 via binding with VEGF-activated β3 integrin. Overexpression of ROBO4 reduces the augmented VEGF-induced angiogenic signal and decreases cerebral neovascularisation in diabetes. Inhibition of the VEGF angiogenic signal by SKLB1002, a selective VEGFR-2 antagonist, decreases ROBO4–β3 integrin interaction, increases the expression and availability of ROBO4 and prevents/repairs cerebral neovascularisation in diabetes

**Table 1**

Rat metabolic characteristics

| Characteristic | GK | | GK+SLKB1002 | |
|---|---|---|---|---|
| | 12 weeks | 16 weeks | 12 weeks | 16 weeks |
| Body weight (g) | 257±8 | 362±5 | 268±8 | 346±6 |
| Blood glucose (mmol/l) | 10.66±1.22 | 13.94±0.77 | 9.61±0.55 | 11.44±1.11 |
| $HbA_{1c}$ (%) | 7.3±0.6 | 8.4±0.25 | 7.6±0.5 | 7.8±0.4 |
| $HbA_{1c}$ (mmol/mol) | 56±9 | 68±3 | 60±5 | 62±4 |
| Albuminuria[a] | – | – | – | + |

[a]–, albuminuria scored as null; +, 20 mg/l albuminuria